European Journal of Radiology 110 (2019) 30–38

Contents lists available at ScienceDirect

European Journal of Radiology

journal homepage: www.elsevier.com/locate/ejrad

Research article

A nomogram for individual prediction of vascular invasion in primary breast cancer

Fu-sheng Ouyang[a,1], Bao-liang Guo[a,1], Xi-yi Huang[b,1], Li-zhu Ouyang[c,1], Cui-ru Zhou[a], Rong Zhang[a], Mei-lian Wu[a], Zun-shuai Yang[a], Shang-kun Wu[a], Tian-di Guo[a], Shao-ming Yang[a,*], Qiu-gen Hu[a,*]

[a] Department of Radiology, Shunde Hospital of Southern Medical University, Foshan, Guangdong, PR China
[b] Department of Laboratory, Lecong Hospital of Shunde, Foshan, Guangdong, PR China
[c] Department of Ultrasound, Shunde Hospital of Southern Medical University, Foshan, Guangdong, PR China

ARTICLE INFO

Keywords:
Breast cancer
Magnetic Resonance Imaging
Vascular invasion
Nomogram

ABSTRACT

Objectives: To explore the feasibility of preoperative prediction of vascular invasion (VI) in breast cancer patients using nomogram based on multiparametric MRI and pathological reports.

Methods: We retrospectively collected 200 patients with confirmed breast cancer between January 2016 and January 2018. All patients underwent MRI examinations before the surgery. VI was identified by postoperative pathology. The 200 patients were randomly divided into training (n = 100) and validation datasets (n = 100) at a ratio of 1:1. Least absolute shrinkage and selection operator (LASSO) regression was used to select predictors most associated with VI of breast cancer. A nomogram was constructed to calculate the area under the curve (AUC) of receiver operating characteristics, sensitivity, specificity, accuracy, positive prediction value (PPV) and negative prediction value (NPV). We bootstrapped the data for 2000 times without setting the random seed to obtain corrected results.

Results: VI was observed in 79 patients (39.5%). LASSO selected 10 predictors associated with VI. In the training dataset, the AUC for nomogram was 0.94 (95% confidence interval [CI]: 0.89–0.99, the sensitivity was 78.9% (95%CI: 72.4%–89.1%), the specificity was 95.3% (95%CI: 89.1%–100.0%), the accuracy was 86.0% (95%CI: 82.0%–92.0%), the PPV was 95.7% (95%CI: 90.0%–100.0%), and the NPV was 77.4% (95%CI: 67.8%–87.0%). In the validation dataset, the AUC for nomogram was 0.89 (95%CI: 0.83–0.95), the sensitivity was 70.3% (95%CI: 60.7%–79.2%), the specificity was 88.9% (95%CI: 80.0%–97.1%), the accuracy was 77.0% (95%CI: 70.0%–83.0%), the PPV was 91.8% (95%CI: 85.3%–98.0%), and the NPV was 62.7% (95%CI: 51.7%–74.0%). The nomogram calibration curve shows good agreement between the predicted probability and the actual probability.

Conclusion: The proposed nomogram could be used to predict VI in breast cancer patients, which was helpful for clinical decision-making.

1. Introduction

Breast cancer is one of the most common malignant tumors among women world widely. A correct identification of poor prognostic factors for breast cancer may help guiding more aggressive adjuvant treatment protocols [1]. Identification of simple and measurable prognostic factors is an important issue in clinical decision-making of breast cancer [2]. Ideal prognostic factors would be capable of predicting the short survival in some patients [3]. The major cause of short survival in breast cancer is dispersion of malignant cells from the primary location leading to formation of metastases [4].

One of the important steps in metastasis is the invasion of vascular

Abbreviations: LASSO, least absolute shrinkage and selection operator; AUC, area under the curve; CI, confidence Interval; PPV, positive prediction value; NPV, negative prediction value; DCE, dynamic contrast-enhanced; DWI, diffusion-weighted imaging; ALNM, axillary lymph node metastasis; TIC, time-intensity curve; ER, estrogen receptor; PR, progesterone receptor; HER2, human epidermal growth factor receptor; LVI, lymphovascular invasion; LI, lymphatic invasion; VI, vascular invasion; IDC, invasive ductal carcinoma

* Corresponding authors at: No. 1, Penglai Road, Daliang District, Shunde, Foshan, Guangdong, PR China.
E-mail addresses: shaominyang@126.com (S.-m. Yang), qiugenhu@126.com (Q.-g. Hu).

[1] These authors contributed equally to this work.

https://doi.org/10.1016/j.ejrad.2018.11.013
Received 25 August 2018; Received in revised form 12 November 2018; Accepted 13 November 2018

spaces (lymphatic and/or blood vessel) by tumoral cells, i.e. tumor cells spreading through the lymphatic or blood vascular networks [5]. Peritumoral vascular invasion (VI) is considered to be an early step in the metastatic process and a key hallmark of aggressiveness tumors, therefore is very important for the progress of malignant tumors [6]. When examined on tissue sections as a morphologic marker, the presence of VI is a strong prognostic factor in many tumors, such as colonic, bladder and cervical carcinomas [7–9]. It has also been shown that VI is positively correlated with regional lymph node metastasis and a greater recurrence rate in such cancers [10,11]. A study also showed the presence of VI could be considered as an indicator of high biological aggressiveness, which may be a strong prognostic factor in breast cancer [2]. Accurate identification of VI in breast cancer patients is crucial for prognosis and treatment strategy decisions. However, VI is only available postoperatively. Preoperative knowledge of VI can provide valuable information for determining the need for adjuvant therapy, thus aiding in clinical decision making. Therefore, from a clinical point of view, predicting VI in breast cancer before surgery would benefit further management of patients, which is valuable and urgently needed.

To predict VI in breast cancer, potential factors associated with VI in various aspects should be taken into consideration. Anatomical MRI can provide morphological information of breast tumor (e.g., size, margins, and location) and axillar lymph nodes. Diffusion-weighted imaging (DWI) in a fast time acquisition and without contrast medium gives information about cellularity of breast cancer [12]. Perfusion can give additional information as regards vascularization of breast cancer [13]. In addition, clinical parameters such as estrogen receptor (ER), progesterone receptor (PR), human epidermal growth factor receptor (HER2), and Ki-67 proliferation could provide an insight into the functional activity of receptors and tumor proliferation.

Therefore, the present study aims to individually predict VI in breast cancer and develop a quantitative model for the assessment of VI based on clinical, multiparametric MRI and pathologic parameters before treatment, which will facilitate clinical decision-making of breast cancer.

2. Materials and methods

2.1. Basic characteristics of patients

This present study was approved by the Ethics Committee of our hospital, and the patient's informed consent was waived. We retrospectively investigated the cases of 200 consecutive patients with single primary breast cancer admitted to our department from January 2016 to January 2018. All patients underwent a 1.5 T MRI examination before 16 G or 18 G needle core biopsy and surgery. Patients with previously-diagnosed breast cancer or incomplete clinical information were excluded, and male patients were excluded as well. None of the patients had received preoperative chemotherapy. In this study, we defined VI as the presence of tumor cells in the peritumoral vascular channels based on postoperative pathology. VI was recorded as being present or absent. Clinical information was collected including age, ER, PR, HER2, Ki-67 labeling index and histological type [e.g., invasive ductal carcinoma (IDC) (histological grade 1), IDC (histological grade 2), IDC (histological grade 3), ductal carcinoma in situ and neuroendocrine carcinoma]. ER, PR, HER2, Ki-67-labeling index and histological type were confirmed by needle core biopsy. MR imaging features included breast density (fatty, dense or mixed), location (upper-outer quadrant, upper-inner quadrant, lower-outer quadrant, lower-inner quadrant, or central position), tumor size (maximum diameter), margins (well- defined or ill- defined), lobulation sign (absence or presence), spiculation sign (absence or presence), MRI- reported axillary lymph node metastasis (ALNM) (absent, single or multiple), contrast enhancement patterns (obvious enhancement or slight enhancement), DWI appearance (marked hyperintensity or slight hyperintensity), time-intensity curve (TIC) patterns (type I, a straight or curved line; type II, a sharp bend after the initial upslope with plateau thereafter; type III, contrast washout was evident after an initial upslope). The MR imaging features were retrospectively reviewed by two independent radiologists with more than 10 years of experience in breast imaging, and who were blinded to the pathology reports.

2.2. MR image acquisition

The MR imaging was performed in the prone position using a dedicated eight-channel double-breast coil with a 1.5 T system (Achieva, Philips Medical Systems, Nederland B.V.). Bilateral whole-breast MR imaging was performed using the following sequences and parameters: axial T1-weighted Turbo Spin Echo (TSE) (TR/TE = 486 ms/10 ms, section thickness = 3 mm, matrix = 200 × 189, FOV = 220 × 286 mm). Axial T2-weighted spectrally selective attenuated inversion recovery (SPAIR) (TR/TE = 4132 ms/120 ms, section thickness = 3 mm, matrix = 312 × 288, FOV = 250 × 301 mm). Axial DWI was obtained with gradient echo planar imaging (GRE-EPI) sequence (TR/TE = 2896 ms/66 ms, section thickness = 3 mm, matrix = 120 × 75, FOV = 365 × 231 mm, b value = 0, 1000s/mm^2). Dynamic Contrast-Enhanced (DCE) Magnetic Resonance Imaging was performed using the high resolution isotropic volume excitation (e-THRIVE) (TR/TE = 6.0 ms/2.9 ms, flip angle = 10°, matrix = 252 × 243, FOV = 350 × 256 × 150 mm, voxel size = 1.4 × 1.05 × 1 mm^3). For DCE images, a bolus of 0.1 mmol kg^{-1} of gadodiamide (Omniscan, GE Healthcare) was injected into the antecubital vein at a rate of 3 mL/s, followed by a 16 mL saline flush. Dynamic axial MR images were obtained once before and five times after the administration of contrast agent at 50 s intervals. For analysis of enhancement kinetics, TICs were plotted based on the signal intensity values obtained in the regions of interest (ROI) on serial dynamic images.

2.3. Pathologic assessment

Immunohistochemical staining was performed using streptavidin-peroxidase. The pathological report from the initial breast biopsy was used to record the ER, PR, HER2 status, Ki-67-labeling index and histological type of each breast cancer. Samples were scored as positive for ER or PR by immunohistochemistry when at least 1% of the tumor cell nuclei showed staining for ER or PR, respectively [14]. When membrane staining is observed in > 10% of tumor cells, HER2 is positive, and if less than 10% membrane staining is observed then HER2 is negative [15]. The Ki-67-labeling index is defined as the percentage of positively stained tumor cells among the total number of malignant cells assessed [16]. Histological types were recorded, including but not limit to IDC (histological grades 1–3), ductal carcinoma in situ, and neuroendocrine carcinoma.

2.4. Clinical, pathologic and radiological feature selection

We used the least absolute shrinkage and selection operator (LASSO) logistic regression to select the most significant features from the training dataset. LASSO-penalty is a popular variable selection method that used in many previous studies [17–19]. The LASSO-penalty estimate is defined by

$$\hat{\beta}^{lasso} = \underset{\beta}{\operatorname{argmin}} \sum_{i=1}^{N} \left(y_i - \beta_0 - \sum_{j=1}^{p} x_{ij}\beta_j\right)^2 \quad \text{subject to } \sum_{j=1}^{p} |\beta_j| \le t$$

We can re-parametrize the constant by standardizing the predictors; the solution for $\hat{\beta}_0$ is $\bar{y}$, and thereafter we fit a model without an intercept. In the signal processing literature, the lasso is also known as basis pursuit.

We can also write the lasso problem in the equivalent Lagrangian

Table 1
Comparison of clinicopathologic and radiological features between patients with VI and without VI in training dataset and validation dataset.

Parameters	No. of patients with VI (n = 79)	No. of patients without VI (n = 121)	*P* value*
Age	48.9 ± 12.5	49.4 ± 10.5	0.781
Breast density			
Dense (n = 41)	20 (25.3)	21 (17.4)	< 0.001
Fatty (n = 108)	40 (50.6)	68 (56.2)	
lirregular (n = 647)			
Mixed (n = 51)	19 (24.1)	32 (26.4)	
Tumor location			
Upper-outer quadrant (n = 103)	37 (46.8)	66 (54.5)	0.044
Lower-outer quadrant (n = 26)	11 (13.9)	15 (12.4)	
Upper-inner quadrant (n = 43)	13 (16.5)	30 (24.8)	
Lower-inner quadrant (n = 9)	5 (6.3)	4 (3.3)	
quadrant (n = 31)			
Central position (n = 19)	13 (16.5)	6 (5.0)	
Tumor size (maximum diameter, mm)	35.5 ± 17.8	29.1 ± 13.0	0.007
Margins			
Well-defined (n = 59)	1 (1.3)	58 (47.9)	< 0.001
Ill-defined (n = 141)	78 (98.7)	63 (52.1)	
Lobulation sign)			
Hyperechogenicity (n = 61			
Absence (n = 107)	22 (27.8)	85 (70.2)	< 0.001
Presence (n = 93)	57 (72.2)	36 (29.8)	
Spiculation sign			
Absence (n = 102)	30 (38.0)	49 (40.5)	0.721
Presence (n = 98)	49 (62.0)	72 (59.5)	
ALNM			
Absent (n = 48)	17 (21.5)	31 (25.6)	< 0.001
Single (n = 88)	18 (22.8)	70 (57.9)	
Multiple (n = 64)	44 (55.7)	20 (16.5)	
Contrast enhancement pattern patterns			
Obvious enhancement (n = 181)	78 (98.7)	103 (85.1)	0.001
Slight enhancement (n = 19)	1 (1.3)	18 (14.9)	
DWI appearance			
Slight hyperintensity (n = 53)	6 (7.6)	48 (39.7)	< 0.001
Marked hyperintensity (n = 146)	73 (92.4)	73 (60.3)	
TIC pattern			
Type I (n = 15)	0	15 (12.4)	< 0.001
Type II (n = 68)	55 (69.6)	13 (10.7)	
Type III (n = 117)	24 (30.4)	93 (76.9)	
ER	55.6 ± 39.7	55.9 ± 40.9	0.960
PR	30.4 ± 36.8	29.5 ± 37.9	0.866
HER2	1.96 ± 0.79	1.83 ± 0.92	0.270
Ki-67 labeling index index	34.3 ± 24.8	34.1 ± 25.7	0.968
Histological type			
IDC (grade 1) (n = 37)	5 (6.3)	32 (26.4)	< 0.001
IDC (grade 2) (n = 79)	39 (49.4)	40 (33.1)	
IDC (grade 3) (n = 71)	35 (44.3)	36 (29.8)	
Ductal carcinoma in situ (n = 12)	0	12 (9.9)	
Neuroendocrine carcinoma (n = 1)	0	1 (0.8)	

Note: unless otherwise indicated, data are numbers of nodules, and numbers in parentheses are percentages.

* P value were calculated by using generalized estimating equation analysis. DWI = diffusion-weighted imaging; TIC = time-intensity curve; ER = estrogen receptor; PR = progesterone receptor; HER2 = human epidermal growth factor receptor; IDC = invasive ductal carcinoma.

form

$$\hat{\beta}^{lasso} = \underset{\beta}{\operatorname{argmin}} \left\{ \frac{1}{2} \sum_{i=1}^{N} \left(y_i - \beta_0 - \sum_{j=1}^{p} x_{ij}\beta_j \right)^2 + \lambda \sum_{j=1}^{p} |\beta_j| \right\}$$

Notice the similarity to the ridge regression problem: the L_2 ridge penalty $\sum_i^p \beta_j^2$ is replaced by the L1 lasso penalty $\sum_i^p |\beta_j|$. This latter constraint makes the solutions nonlinear in the yi, and there is no closed form expression as in ridge regression. Computing the lasso solution is a quadratic programming problem, although we see that efficient algorithms are available for computing the entire path of solutions as λ is varied, with the same computational cost as for ridge regression. Because of the nature of the constraint, making t sufficiently small will cause most of the coefficients to be exactly zero, and the remaining nonzero coefficients were selected by LASSO.

2.5. Development of an individualized prediction model

Nomograms are statistical models that are suited ideally to individualizing risk assessment [20]. To provide the clinicians with a quantitative tool to diagnose the individual probability of VI, we built the diagnostic nomogram using the independent predictors selected by LASSO to generate a combined indicator for estimating the probability of VI. The nomogram created in the training dataset was applied to the internal and external validation dataset, and the total point for each case were calculated. The nomogram was performed using the total points as a factor. The nomogram plot provides a visible way to quickly obtain the individual prediction risk for the potential patient.

2.6. Apparent performance of the nomogram in the training dataset and validation dataset

Calibration curves were plotted to assess the calibration of the predictive nomogram [21]. Calibration was assessed by plotting the predicted versus the actual probability for quintiles of the predicted probability of VI. The area under the curve (AUC) of receiver operating characteristics (ROC), sensitivity, specificity, accuracy, positive prediction value (PPV) and negative prediction value (NPV) were measured to quantify the discrimination of the nomogram.

The performance of the internally validated nomogram was tested in the validation dataset. The logistic regression formula formed in the training dataset was applied to all patients of the validation dataset, with total points for each patient calculated. Logistic regression in this dataset was then performed by using the total points as a factor. Finally, the discrimination and calibration curve were derived on the basis of the regression analysis.

2.7. Statistical analysis

Statistical analysis used R software (http://www.R-project.org). The packages were listed as follows: The 'glmnet' package for lasso logistic regression; the 'rms' package for nomogram and calibration curve. The prediction performance of nomogram was assessed using the AUC, sensitivity, specificity, accuracy, PPV and NPV. Comparison of clinicopathologic and radiological features between positive VI group and negative VI group in training dataset and validation dataset using independent sample *t*-test or Mann-Whitney U test or Chi-square test. All statistics are two-tailed, and p-value less than 0.05 are considered statistically significant.

3. Results

3.1. Patient characteristics

A total of 200 consecutive breast cancer patients were included, with a mean age of 49.1 ± 11.3 years, ranging from 30 to 78 years.

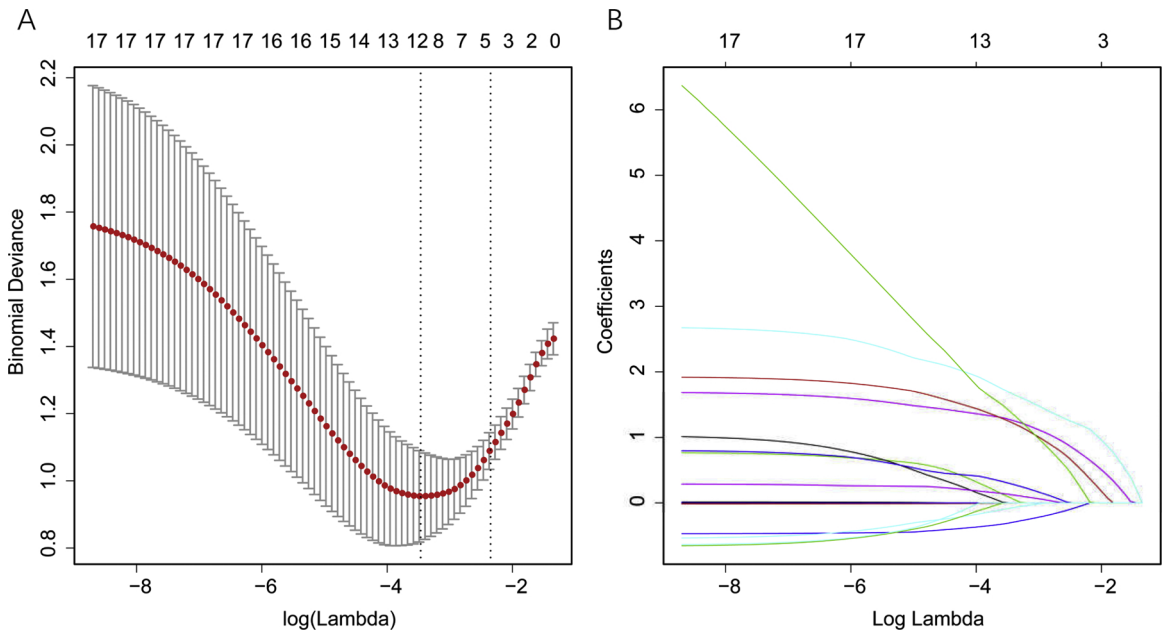

Fig. 1. Clinicopathologic and radiological feature selection using the least absolute shrinkage and selection operator (LASSO) logistic regression model. (A) Identification of the optimal penalization coefficient lambda (λ) in the LASSO model used 10-fold cross-validation and the minimum criterion. As a result, a λ value of 0.030, with log (λ) = −3.49, was selected. (B) LASSO coefficient profiles of the 16 features. The dotted vertical line was plotted at the value selected using 10-fold cross-validation in Fig. 1A, for which the optimal λ resulted in 10 non-zero coefficients.

Among them, 71 (35.5%) were IDC (histological grade 3), 79 (39.5%) were IDC (histological grade 2), 37 (18.5%) were IDC (histological grade 1), 12 (6.0%) were ductal carcinomas in situ, and 1 (0.5%) were neuroendocrine carcinomas. VI was observed in 79 (39.5%) patients, of which, 35 (44.3%) were IDC (histological grade 3), 39 (49.4%) were IDC (histological grade 2), and 5 (6.3%) were IDC (histological grade 1). Comparison of clinicopathologic and radiological features between breast cancer patients with VI and without VI in training dataset and validation dataset was shown in Table 1.

3.2. Predictive factor selection

LASSO regression identified 10 predictors associated with VI out from 16 clinicopathologic and radiological features, including breast density, tumor size (maximum diameter), location, margins, lobulation sign, ALNM, contrast enhancement patterns, DWI appearance, TIC patterns, and pathological type (Fig. 1).

3.3. Prediction performance of nomogram

Fig. 2 shows the nomogram based on the 10 predictors of VI (Fig. 2). In the training dataset, the AUC for nomogram was 0.94 (95%CI: 0.89–0.99, the sensitivity was 78.9% (95%CI: 72.4%–89.1%), the specificity was 95.3% (95%CI: 89.1%–100.0%), the accuracy was 86.0% (95%CI: 82.0%–92.0%), the PPV was 95.7% (95%CI: 90.0%–100.0%), and the NPV was 77.4% (95%CI: 67.8%–87.0%) (Fig. 3). In the validation dataset, the AUC for nomogram was 0.89 (95%CI: 0.83–0.95), the sensitivity was 70.3% (95%CI: 60.7%–79.2%), the specificity was 88.9% (95%CI: 80.0%–97.1%), the accuracy was 77.0% (95%CI: 70.0%–83.0%), the PPV was 91.8% (95%CI: 85.3%–98.0%), and the NPV was 62.7% (95%CI: 51.7%–74.0%) (Fig. 3). Fig. 4 shows the histograms of bootstrapped AUC, sensitivity, specificity, PPV, and NPV, from which, the reported CIs were proven meaningful. The calibration curve for the probability of VI in the training and validation datasets demonstrated good agreement between prediction and observation (Fig. 5). The Hosmer-Lemeshow test yielded a nonsignificant statistic (training dataset, p = 0.68 and validation dataset (p = 0.06), which suggested that there was no departure from perfect fit.

3.4. An example of the nomogram in use

For example, patient 1 aged 52 years, who has a tumor in her left mixed density breast, with maximum diameter of 25 mm, location in the lower-inner quadrant, ill-defined margins, presence of lobulation sign, obvious contrast-enhancement, slight hyperintensity on DWI images, type I TIC, and no ALNM (Fig. 6a–f). Biopsy results showed it was a grade 1 IDC. The risk of VI assessed by nomogram was less than 1% (Fig. 6g). Pathology report showed the tumor hadn't VI. Patient 2 aged 55 years, who a tumor in her left fatty density breast, with maximum diameter of 29 mm, location in the upper-outer quadrant, ill-defined margins, presence of lobulation sign, obvious contrast-enhancement, marked hyperintensity on DWI images, type III TIC, and no ALNM (Fig. 6h–m). Biopsy results showed it was a grade 3 IDC. The risk of VI could be calculated to be more than 90% (Fig. 6n). Final pathology report showed this tumor had VI.

4. Discussion

We proposed a novel nomogram based on clinical, pathologic and radiological features to predict VI in breast cancer. The nomogram incorporated 10 most strong predictors including breast density, tumor size (maximum diameter), location, margins, lobulation sign, ALNM, contrast enhancement patterns, DWI appearance, TIC patterns, and pathological type. Our results showed the nomogram had excellent discrimination in both the training dataset and the validation dataset. We developed an easy-to-use, repeated and relatively objective nomogram that facilitated the individualized prediction of VI.

For many years, patient's age, tumor size, axillar lymph node status, histological grade of malignancy, ER, PR and HER2 represented principal factors used for the stratification of breast cancer patients for the

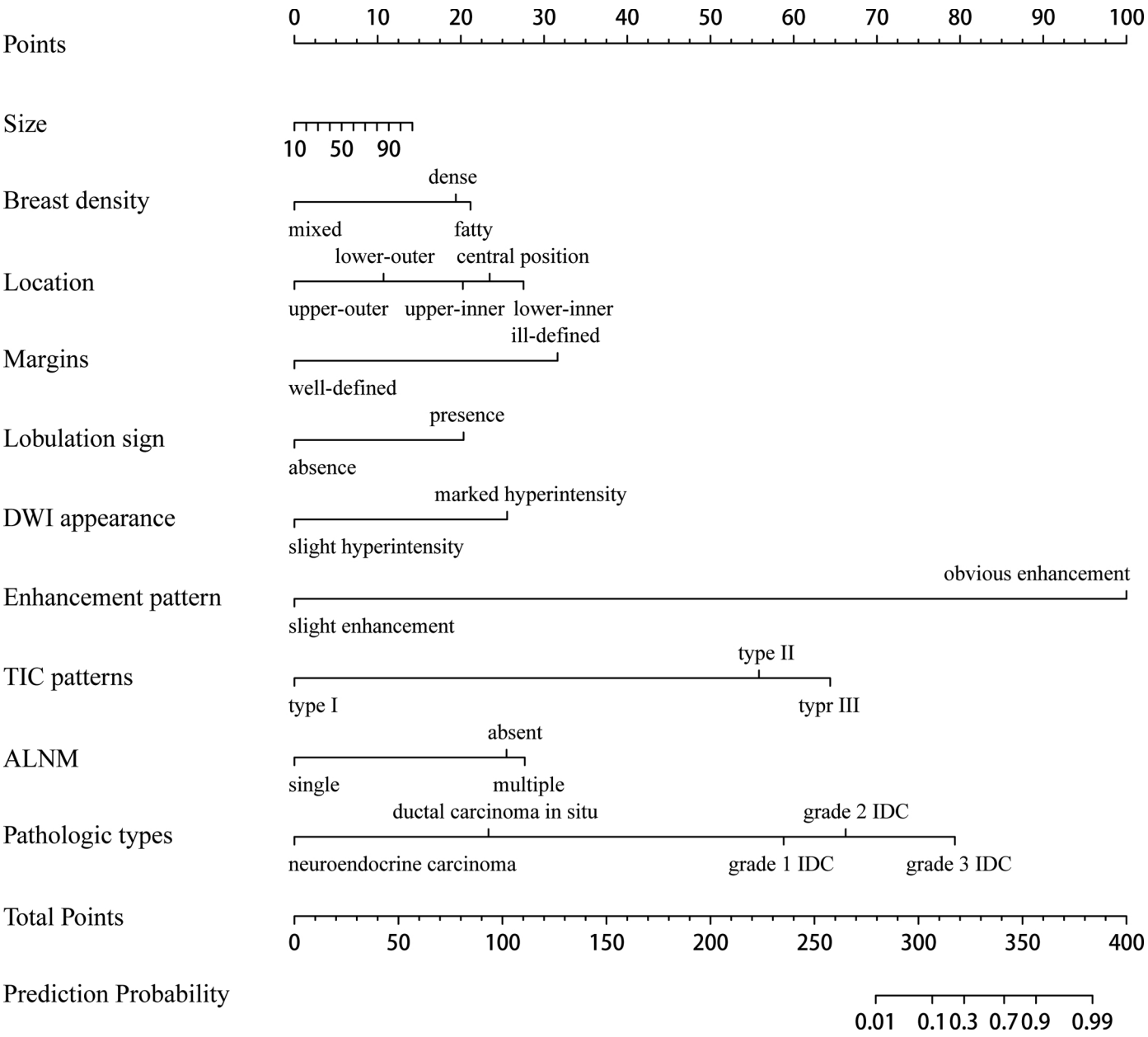

Fig. 2. The nomogram was developed in the training dataset, with the breast density, tumor size (maximum diameter), location, margins, lobulation sign, ALNM, contrast enhancement patterns, DWI appearance, TIC patterns, and pathological type incorporated.

purposes of evaluating the prognosis and determining the appropriate strategy of treatment [22–25]. Lymphovascular invasion (LVI) also has been reported as a strong prognostic factor in patients with breast cancer. Tumor cell invasion of blood vessels or lymphatic vessels is the critical step of tumor cell dissemination and metastasis for predicting disease recurrence or progression. However, most previous studies did not separate LVI into VI and lymphatic invasion (LI) [26–29]. Fujii T et al found the presence of VI, instead of LI, could be an indicator of high biological aggressiveness and may be a valid prognostic factor for breast cancer [5]. Compared to LI, VI may better represent systemic disease due to the strong association between VI and LI [5]. Therefore, to predict systemic disease, it would be helpful to identify the subset of patients with VI among breast cancer patients with or without LI. Patients with VI may require for stronger adjuvant therapies because of the high risk of local, regional, and distant recurrence. However, to our best of knowledge, there was no any study predicted VI in patients with breast cancer before treatment based on available data.

Some studies had showed VI was associated with lower mean age, body weight, breast density, tumor size, positive lymph nodes, and histologic grade [30–32]. Our study found the risk for VI increased with the tumor size. The mean tumor size in patients with VI was larger than that in patients without VI. Some studies have examined the association between breast density and breast cancer characteristics and found breast density was positively associated with tumor size, lymph node status, and VI among women with screen-detected cancers [31,33,34]. We also identified breast density as a predictor of VI, those patients with fatty breast density had higher risk for VI. We observed breast tumor with VI usually had morphological characteristics such as ill-

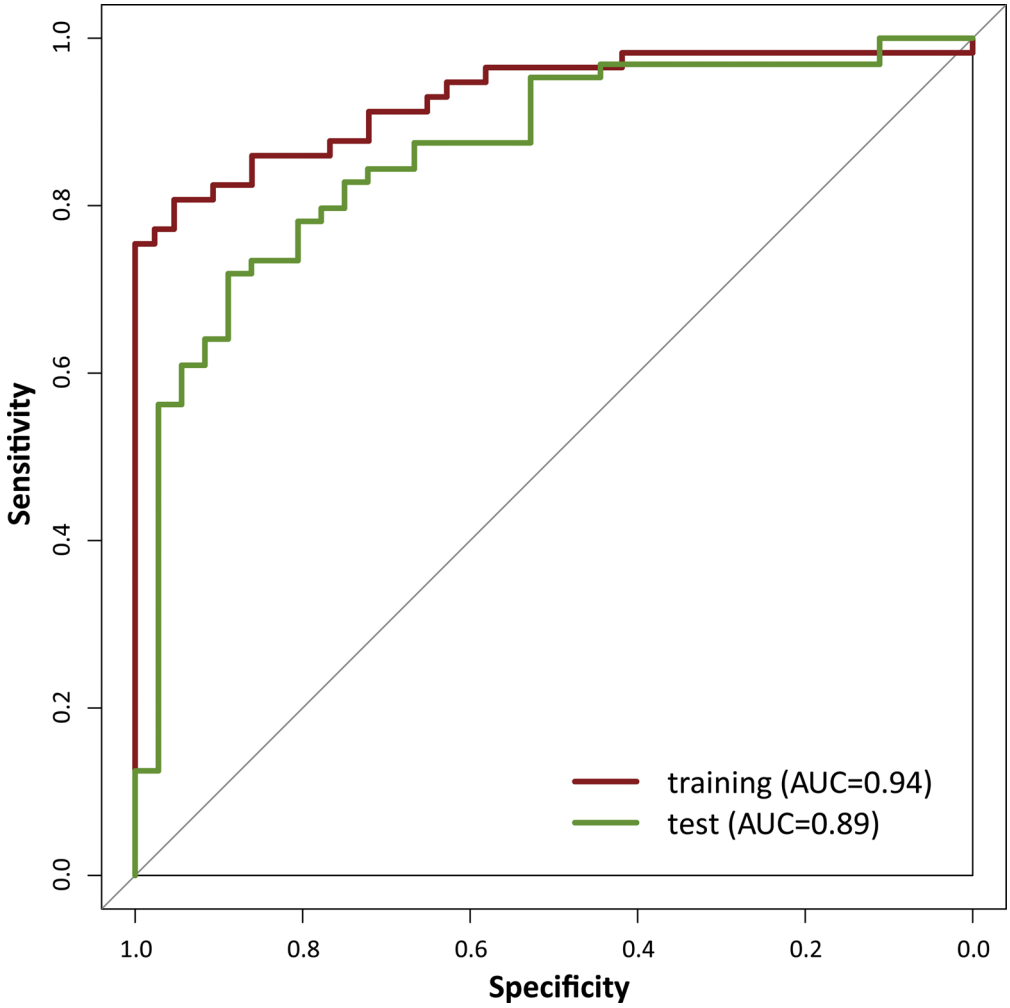

Fig. 3. The ROC curves of the nomogram in the training dataset and validation dataset.

defined margins, lobulation sign, and spiculation sign. In this study, VI was more frequently found in the lower-inner quadrant than other quadrants, which was inconsistent with a previous study. It said may because breast cancer was most likely to occur in the upper-outer quadrant, which was the quadrant with highest breast area and dense area [35]. Analyses from larger trials are warranted to identify this finding. A review has shown that the presence of VI correlates closely with locoregional lymph node involvement [23]. Our study observed VI was associated with ALNM. Multiple ALNM was more common in breast cancer with VI than those without VI (56% vs. 17%, $p < 0.001$). We also noticed pathological type was associated with breast cancer VI. Breast tumors with different pathological types have different biological behavior and therefore have different possibilities of invasion of surrounding tissues. The results showed grade 3 IDC had the highest risk for VI.

It is essential that all MR breast examinations include traditional morphological sequences, complemented by functional imaging techniques which yield information about the underlying pathophysiology of tissue. Functional information of breast tumor could be acquired using DWI and DCE MRI. DWI is an approach that differs from conventional MRI techniques in that is measures the mobility of water within tissues, providing information about tissue cellularity and cell membranes integrity, and it is sensitive to changes in water diffusion in the intracellular and extracellular spaces [36,14]. Restrictions in water diffusion are observed in malignant breast lesions. VI was more frequently observed in tumor with obvious hyperintensity on DWI images. DCE MRI is used to examine neoangiogenically induced vascular changes, which result in the proliferation of abnormally leaky microvessels. Examination of the TICs allows physiological parameters related to tissue perfusion, microvascular vessel wall permeability and extravascular–extracellular volume fraction to be extracted, which may aid characterization of the underlying pathology. Type III TIC was more common in tumor with VI.

Although the variables were useful for the VI prediction in breast cancer patients, their role in determining the individual risk level of the patient and in the selection of supplementary treatment is quite restricted. At present, there is no effective method for accurately predicting tumor VI before surgery. In this study, nomogram was developed based on comprehensive data, with the aim of allowing the clinician to evaluate the risk of VI more accurately, as a tool for determining the appropriate treatment. The proposed predictive model had a trained AUC of 0.94 and an internally validated of 0.89 in ROC curve analysis; internal validation demonstrated good discrimination in predicting VI.

In summary, the nomogram is based on clinical, pathologic and radiological data that can be obtained in a preoperative setting. The proposed nomogram could be used to individually predict VI in breast cancer patients, which was helpful for clinical decision-making.

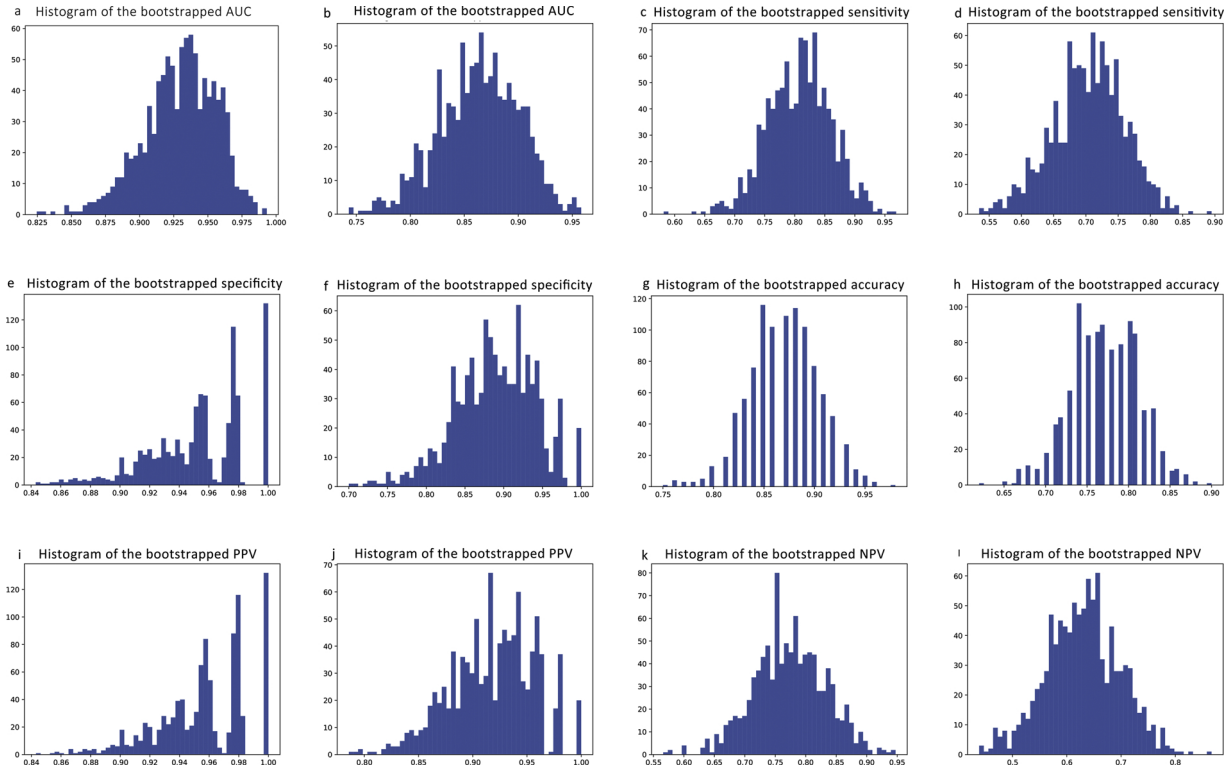

Fig. 4. The histograms of bootstrapped AUC (a–b), sensitivity (c–d), specificity (e–f), accuracy (g–h), PPV (i–j) and NPV (k–l) in the training dataset and validation dataset, from which, the reported CIs were proven meaningful.

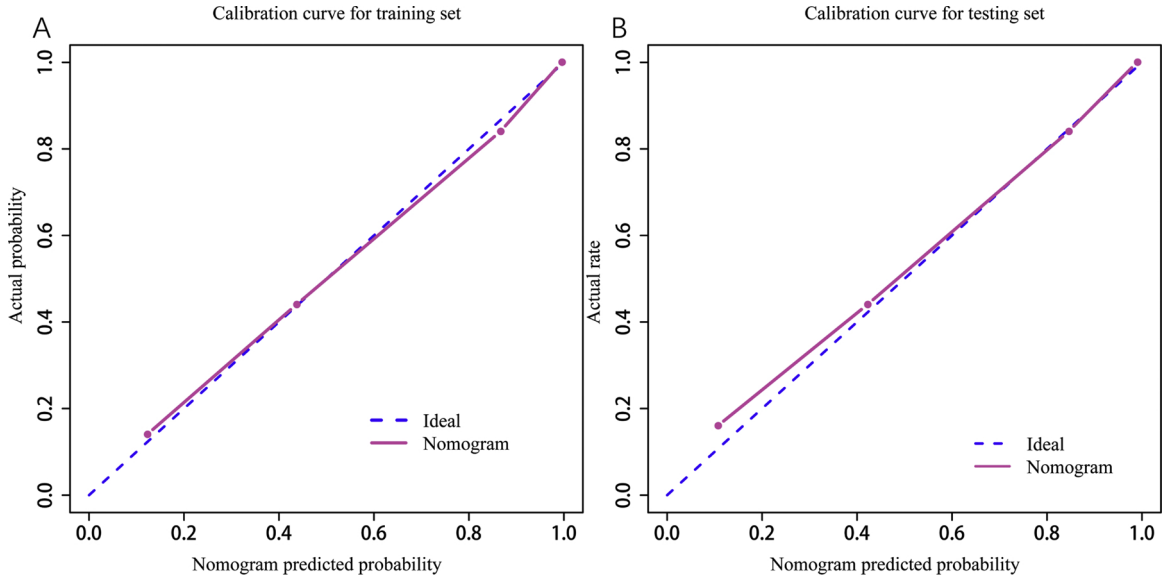

Fig. 5. The calibration curves of the nomogram in the training dataset (A) and validation dataset (B) are reported. The x-axis is the nomogram predicted probability and the y-axis is the actual probability. The prediction performance can be measured by the difference of the fitted curve and slope 1 line (diagonal 45-degree line). The diagonal dotted line represents a perfect prediction by an ideal model. The solid line represents the performance of the nomogram, of which a closer fit to the diagonal dotted line represents a better prediction.

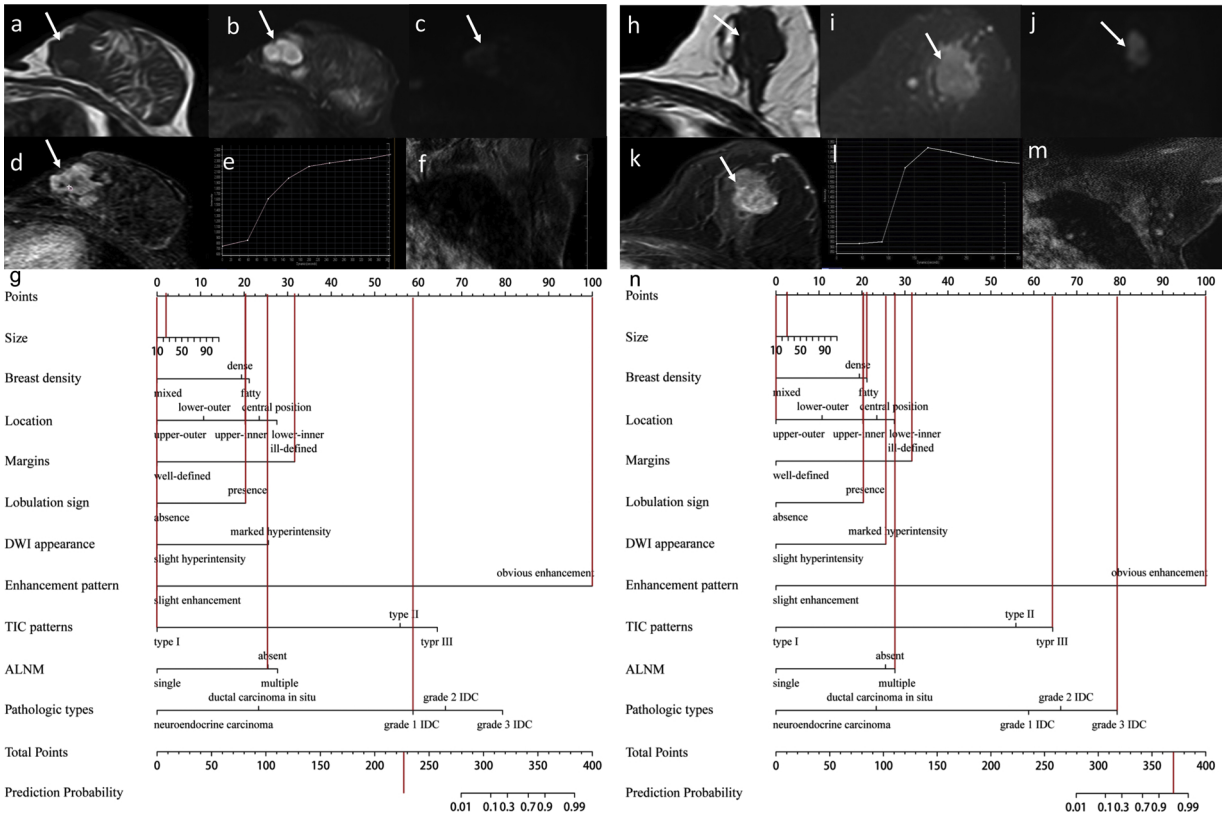

Fig. 6. Examples of the nomogram in use. Breast MRI examinations of patient 1 including axial T1-weighted imaging (a), T2-weighted SPAIR (b), DWI (c), DCE (d), TIC (e) and axillary imaging (f) showed a tumor (white arrows) with size (maximum diameter) of 25 mm, location in the lower-inner quadrant, ill-defined margins, presence of lobulation sign, obvious contrast-enhancement, slight hyperintensity on DWI images, type I TIC, and no ALNM. Biopsy results showed a grade 1 IDC. The risk of VI assessed by nomogram was less than 1% (g). MRI examinations of patient 2 including axial T1-weighted imaging (h), T2-weighted SPAIR (i), DWI (*j*), DCE (k), TIC (l) and axillary imaging (m) showed a tumor (white arrows) with size (maximum diameter) of 29 mm, location in the upper-outer quadrant, ill-defined margins, presence of lobulation sign, obvious contrast-enhancement, marked hyperintensity on DWI images, type III TIC, and no ALNM. Biopsy results showed a grade 3 IDC. The risk of VI could be calculated to be more than 90% (n).

Patients with VI may require for stronger adjuvant therapies because of the high risk of recurrence.

Conflicts of interest

The authors have declared that no conflict of interest exists.

Acknowledgment

This work received funding from the science and technology project of foshan (2017AB003623 and 2017AB003683).

References

[1] I. Mori, Q. Yang, K. Kakudo, Predictive and prognostic markers for invasive breast cancer, Pathol. Int. 52 (2002) 186–194.
[2] A. Rezaianzadeh, A. Talei, A. Rajaeefard, et al., Vascular invasion as an independent prognostic factor in lymph node negative invasive breast cancer, Asian Pac. J. Cancer Prev. 13 (2012) 5767–5772.
[3] B. Kuru, M. Camlibel, M.A. Gulcelik, H. Alagol, Prognostic factors affecting survival and disease-free survival in lymph node-negative breast carcinomas, J. Surg. Oncol. 83 (2003) 167–172.
[4] K. Steinauer, M.W. Gross, D.J. Huang, S. Eppenberger-Castori, U. Guth, Radiotherapy in patients with distant metastatic breast cancer, Radiat. Oncol. 9 (2014) 126.
[5] T. Fujii, R. Yajima, T. Hirakata, et al., Impact of the prognostic value of vascular invasion, but not lymphatic invasion, of the primary tumor in patients with breast cancer, Anticancer Res. 34 (2014) 1255–1259.
[6] M. Mannelqvist, E. Wik, I.M. Stefansson, L.A. Akslen, An 18-gene signature for vascular invasion is associated with aggressive features and reduced survival in breast cancer, PLoS One 9 (2014) e98787.
[7] K. Ichimasa, S.E. Kudo, H. Miyachi, et al., Comparative clinicopathological characteristics of colon and rectal T1 carcinoma, Oncol. Lett. 13 (2017) 805–810.
[8] J.I. Lopez, J.C. Angulo, The prognostic significance of vascular invasion in stage T1 bladder cancer, Histopathology 27 (1995) 27–33.
[9] D. Ertoy, A. Ayhan, E. Sarac, et al., Clinicopathological implication of cripto expression in early stage invasive cervical carcinomas, Eur. J. Cancer 36 (2000) 1002–1007.
[10] S.E. Pinder, I.O. Ellis, M. Galea, S. O'Rouke, R.W. Blamey, C.W. Elston, Pathological prognostic factors in breast cancer. III. Vascular invasion: relationship with recurrence and survival in a large study with long-term follow-up, Histopathology 24 (1994) 41–47.
[11] P.J. Westenend, C.J. Meurs, R.A. Damhuis, Tumour size and vascular invasion predict distant metastasis in stage I breast cancer. Grade distinguishes early and late metastasis, J. Clin. Pathol. 58 (2005) 196–201.
[12] I. Thomassin-Naggara, C. De Bazelaire, J. Chopier, M. Bazot, C. Marsault, I. Trop, Diffusion-weighted MR imaging of the breast: advantages and pitfalls, Eur. J. Radiol. 82 (2013) 435–443.
[13] L.W. Turnbull, Dynamic contrast-enhanced MRI in the diagnosis and management of breast cancer, NMR Biomed. 22 (2009) 28–39.
[14] M. Fan, T. He, P. Zhang, J. Zhang, L. Li, Heterogeneity of diffusion-weighted imaging in tumours and the surrounding stroma for prediction of Ki-67 proliferation status in breast cancer, Sci. Rep. 7 (2017) 2875.
[15] G. Turashvili, S. Leung, D. Turbin, et al., Inter-observer reproducibility of HER2 immunohistochemical assessment and concordance with fluorescent in situ hybridization (FISH): pathologist assessment compared to quantitative image analysis, BMC Cancer 9 (2009) 165.
[16] N. Pathmanathan, R.L. Balleine, Ki67 and proliferation in breast cancer, J. Clin. Pathol. 66 (2013) 512–516.
[17] A. Tahmassebi, A.H. Gandomi, I. McCann, et al., An evolutionary approach for fMRI big data classification, 2017 IEEE Congress on Evolutionary Computation (CEC) (2017) 1029–1036.
[18] A. Tahmassebi, G.J. Wengert, T.H. Helbich, et al., Impact of machine learning with multiparametric magnetic resonance imaging of the breast for early prediction of response to neoadjuvant chemotherapy and survival outcomes in breast cancer

patients, Invest. Radiol. (October) (2018), https://doi.org/10.1097/RLI.0000000000000518 [Epub ahead of print] iii).
[19] A. Tahmassebi, K. Pinker-Domenig, G. Wengert, et al., Determining the importance of parameters extracted from multi-parametric MRI in the early prediction of the response to neo-adjuvant chemotherapy in breast cancer, Med. Imaging 43 (2018).
[20] L. Dihge, P.O. Bendahl, L. Ryden, Nomograms for preoperative prediction of axillary nodal status in breast cancer, Br. J. Surg. 104 (2017) 1494–1505.
[21] B. Zhang, J. Tian, D. Dong, et al., Radiomics features of multiparametric MRI as novel prognostic factors in advanced nasopharyngeal carcinoma, Clin. Cancer Res. 23 (2017) 4259–4269.
[22] A. Morabito, E. Magnani, M. Gion, et al., Prognostic and predictive indicators in operable breast cancer, Clin. Breast Cancer 3 (2003) 381–390.
[23] R.S. Rampaul, S.E. Pinder, C.W. Elston, I.O. Ellis, Prognostic and predictive factors in primary breast cancer and their role in patient management: the Nottingham Breast Team, Eur. J. Surg. Oncol. 27 (2001) 229–238.
[24] A. Kapoor, V.G. Vogel, Prognostic factors for breast cancer and their use in the clinical setting, Expert Rev. Anticancer Ther. 5 (2005) 269–281.
[25] J. Huober, S. Gelber, A. Goldhirsch, et al., Prognosis of medullary breast cancer: analysis of 13 International Breast Cancer study Group (IBCSG) trials, Ann. Oncol. 23 (2012) 2843–2851.
[26] E.A. Rakha, S. Martin, A.H. Lee, et al., The prognostic significance of lymphovascular invasion in invasive breast carcinoma, Cancer-Am. Cancer Soc. 118 (2012) 3670–3680.
[27] Y.J. Song, S.H. Shin, J.S. Cho, M.H. Park, J.H. Yoon, Y.J. Jegal, The role of lymphovascular invasion as a prognostic factor in patients with lymph node-positive operable invasive breast cancer, J. Breast Cancer 14 (2011) 198–203.
[28] A.H. Lee, S.E. Pinder, R.D. Macmillan, et al., Prognostic value of lymphovascular invasion in women with lymph node negative invasive breast carcinoma, Eur. J. Cancer 42 (2006) 357–362.
[29] B. Ejlertsen, M.B. Jensen, F. Rank, et al., Population-based study of peritumoral lymphovascular invasion and outcome among patients with operable breast cancer, J. Natl. Cancer Inst. 101 (2009) 729–735.
[30] R.A. Badwe, I.S. Fentiman, R.R. Millis, W.M. Gregory, Body weight and vascular invasion in post-menopausal women with breast cancer, Br. J. Cancer 75 (1997) 910–913.
[31] E.J. Aiello, D.S. Buist, E. White, P.L. Porter, Association between mammographic breast density and breast cancer tumor characteristics, Cancer Epidemiol. Biomark. Prev. 14 (2005) 662–668.
[32] K.T. Hwang, Y.A. Kim, J. Kim, et al., The influences of peritumoral lymphatic invasion and vascular invasion on the survival and recurrence according to the molecular subtypes of breast cancer, Breast Cancer Res. Treat. 163 (2017) 71–82.
[33] M.A. Roubidoux, J.E. Bailey, L.A. Wray, M.A. Helvie, Invasive cancers detected after breast cancer screening yielded a negative result: relationship of mammographic density to tumor prognostic factors, Radiology 230 (2004) 42–48.
[34] E. Sala, L. Solomon, R. Warren, et al., Size, node status and grade of breast tumours: association with mammographic parenchymal patterns, Eur. Radiol. 10 (2000) 157–161.
[35] S. Chan, J.H. Chen, S. Li, et al., Evaluation of the association between quantitative mammographic density and breast cancer occurred in different quadrants, BMC Cancer 17 (2017) 274.
[36] D.A. Hamstra, A. Rehemtulla, B.D. Ross, Diffusion magnetic resonance imaging: a biomarker for treatment response in oncology, J. Clin. Oncol. 25 (2007) 4104–4109.